ISSN 1669- 3264

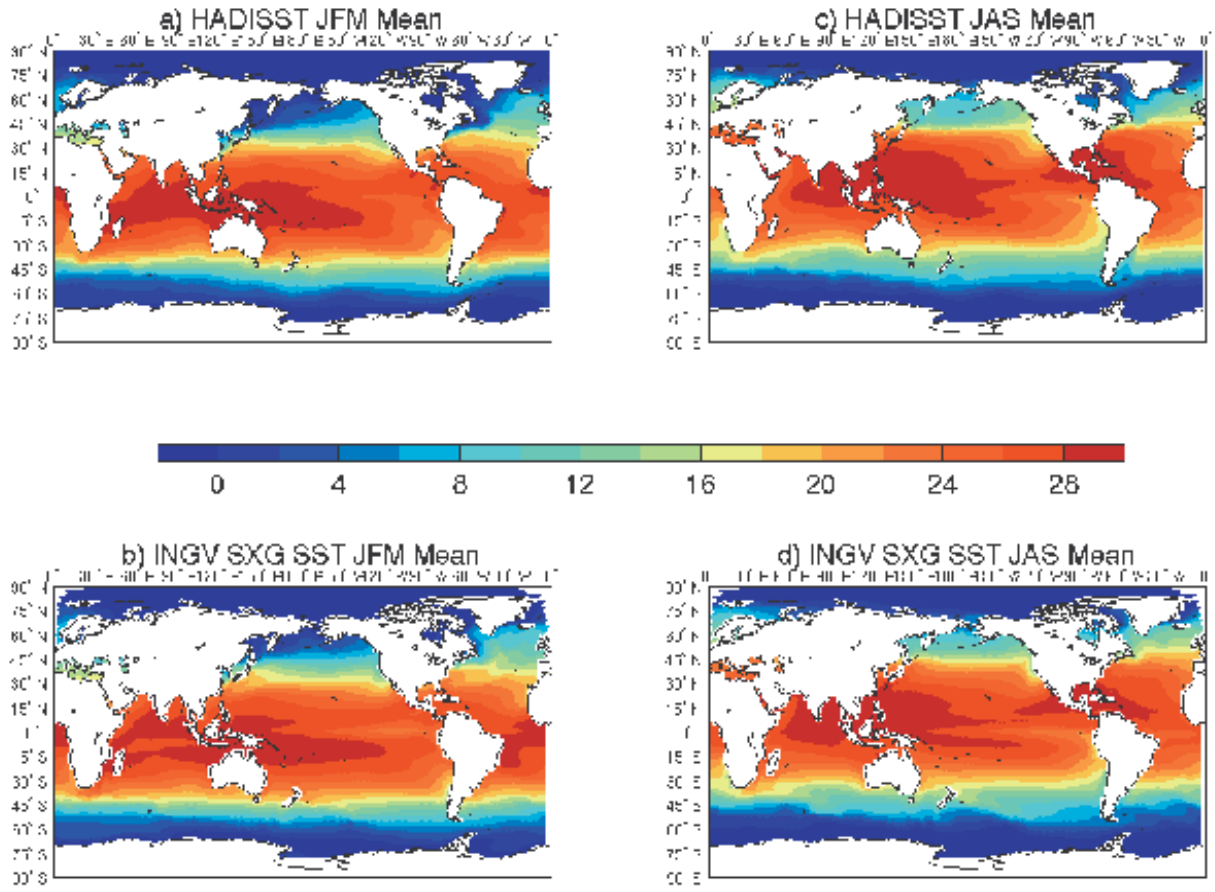

Figure 2: mean sea-surface temperature (SST). Left panels (a and b) northern winter (January-February-March) means; right panels (c and d) northern summer (July,August-September) means. Upper panels (a and c) observations (HadISST data set), the mean field has been obtained by averaging over the 1958-2000 period. Bottom panels (b and d) SXG model simulation: the mean has been obtained by averaging over the simulated 1958-2000 period. Contour is 2 °C. (see art.on page XX)

CLARIS NEWS

The Newsletter of the **European Project of the 6th Framework programme**

A Europe-South America Network for Climate Change Assessment and Impact Studies

Issue 4 - June 2006

The CLARIS Project is coordinated by

EDITORIAL

Dear Colleagues,

The CLARIS project is reaching its second anniversary. Our 2nd year meeting in Paris (21st to 23rd of June) is the opportunity to evaluate the first achievements of the project, to identify its weaknesses, and to initiate a common reflection on the scientific themes, which motivated the network, as well as on its future prospects. Thus, during the 2nd year meeting, major emphasis will be put on scientific discussions around the themes of «Climate modeling», «Extreme events: observing, analyzing and modeling» and «Climate and Society».

Rather than duplicating efforts already done in other programs or panels (such as VAMOS or MESA), our reflection is aimed at highlighting how the Europe-South America collaboration can be most valuable as to supporting specific international recommendations or promoting new approaches.

The CLARIS project 2nd year has been very rich in new progress and results. First, two major training activities were organized in the Department of Atmosphere and Ocean Sciences of the University of Buenos Aires. The CLARIS project is thankful to the Department for letting us using their facilities on both occasions. The first training activity, called «Climate variability studies based on Matlab applications», was delivered by Enrico Scoccimarro and Andrea Carril from INGV in February 2006. The course raised such interest that a second one will be held in August. This issue of the Newsletter contains a summary of the course. The second training activity organized by Marcello Donatelli from CRA-ISCI in March 2006 aimed at forming students, researchers and agronomists in the use of the CROPSYST model. Many agronomists from INTA participated in the course.

Second, the CLARIS Downscaling Group (WP3.1) led by Claudio Menendez and Manuel Castro completed the extreme event simulations providing a first analysis of several regional model performances and their potential parameterization improvements. Given the amount of information and the need for scientific discussions expressed by the group, a special extra-day meeting will be organized on Tuesday 20th of June in Paris.

Third, the CLARIS Dataserver storage capacity has been expanded to more than 4To by acquiring a RAID system. Thus, the CLARIS Dataserver is able to offer to the CLARIS participants the opportunity to continue storing specific IPCC simulations as well as outputs of the downscaling experiments realized in the WP3.1 framework. Moreover, the CLARIS Dataserver now offers new services such as the LAS interface that makes is possible to visualize observations and model outputs stored on the server.

Fourth, the CLARIS daily database is now operational. It is important to point out that the efforts of the Working group 3.2 have been well received during a GCOS/WCRP meeting in Switzerland where Matilde Rusticucci presented the database status. Not only the meeting supported the creation and development of such database, but they also encouraged other countries to contribute to the database and to make their data openly available.

Finally, the groups on impacts (agriculture and health) have calibrated their impact models during the 2nd year and will perform climate change simulations during the last year of the CLARIS project.

I hope you will enjoy reading this fourth issue of the CLARIS Newsletter.
Sincerely yours,

Jean-Philippe Boulanger

WP3.2: Report on data availability, quality-control methods and perspectives

Matilde Rusticucci
Departamento de Ciencias de la Atmósfera y los Océanos, UBA

The CLARIS Daily Data Base has been incorporating new data this year. At the moment we have daily maximum and minimum temperatures and precipitation from 98 stations. CLARIS partners from Uruguay, Brazil and Chile have obtained the data from their Weather Services to make them available for CLARIS studies. The longest records start in 1950, the majority in the 60´s.

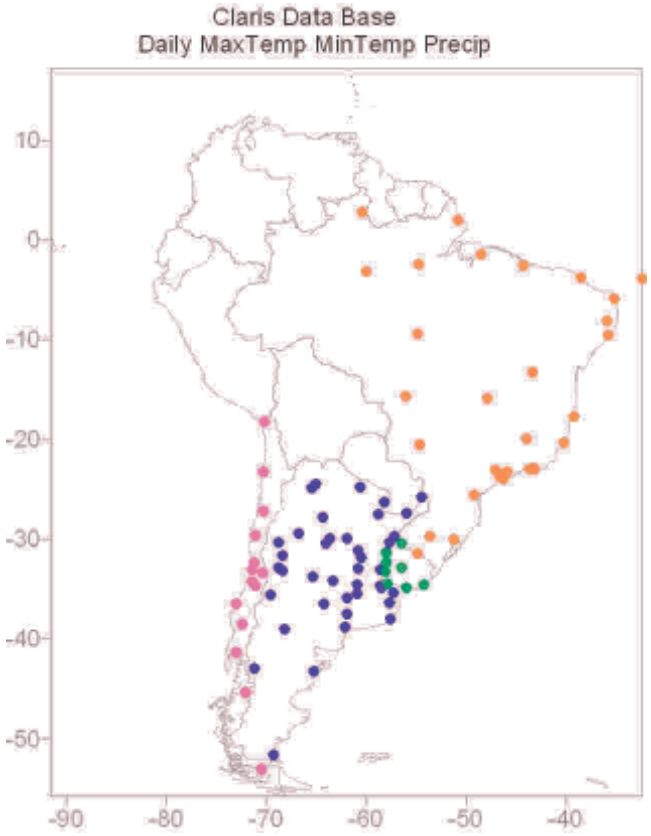

CLARIS Database: Daily Maximum and Minimun Temperature and Precipitation

We are now checking the quality of data, applying the same quality controls to these new stations, as Barrucand and Rusticucci (2001) applied to the temperatures over Argentina and Penalba (personal communication) applied to Argentina precipitation data. Rusticucci and Renom (2005) have already done these controls to the temperatures of Uruguay.
With these strict controls we expect to obtain a homogeneously controlled daily database in the region. This is the first step to estimate homogeneous regional indices which is the next deliverable of our WP.
The CLARIS data base status was presented by Matilde Rusticucci (WP3.2 leader) at the GCOS (Global Climate Observing System) /WCRP Atmospheric Observation Panel for Climate. She has been invited to assist to the Ttwelfth session held in Geneva, Switzerland on 3 – 7 April 2006. Our efforts were received with great interest and the following recommendation was included in the AOPC-XII: CONSOLIDATED LIST OF CONCLUSIONS: The AOPC commended the progress being made in the CLARIS (Europe-South America Network for Climate Change Assessment and Impact Studies) project to assemble data from a number of countries in South America. It encouraged additional countries to contribute data to this effort and to make them openly available for climate monitoring purposes.
(http://www.wmo.ch/web/gcos/Publications/gcos-105.pdf)
This 'encouragement' to make the database openly available exceeds our objectives, but it is undoubtedly a challenge for data-users researchers.

A Bayesian approach for multi-model downscaling: Seasonal forecasting of regional rainfall and river flows in South America

C. A. S. Coelho and D. B. Stephenson
Department of Meteorology, University of Reading, U.K.
e-mail: c.a.d.s.coelho@reading.ac.uk
F. J. Doblas-Reyes and M. Balmaseda
European Centre for Medium-Range Weather Forecast, U.K.
***A. Guetter**, Instituto Tecnológico SIMEPAR, Centro Politécnico da UFPR, Brazil*
***G. J. van Oldenborgh**, Royal Dutch Meteorological Institute, The Netherlands*

This study addresses three issues: spatial downscaling, calibration, and combination of seasonal predictions produced by different coupled ocean-atmosphere climate models. It examines the feasibility of using a Bayesian procedure for producing combined, well-calibrated downscaled seasonal rainfall forecasts for two regions in South America (Figure 1) and river flow forecasts for the Paraná river in the south of Brazil and the Tocantins river in the north of Brazil (Figure 1).

Forecast		MSE [mm^2]	Correlation	Uncertainty [mm]	Brier Score
South box:	Multi-model	0.37	0.57	0.39	0.22
	Forecast Assimilation	0.21	0.74	0.42	0.17
North box:	Multi-model	0.43	0.62	0.49	0.21
	Forecast Assimilation	0.39	0.63	0.55	0.18

Table 1. Skill and uncertainty measures of 3-month lead November-December-January 1959-2001 rainfall anomaly predictions for the two boxes defined in Figure 1. Mean squared error (MSE) in mm^2, correlation, mean predicted uncertainty in mm, Brier score for the event 'rainfall anomaly less than or equal to zero'.

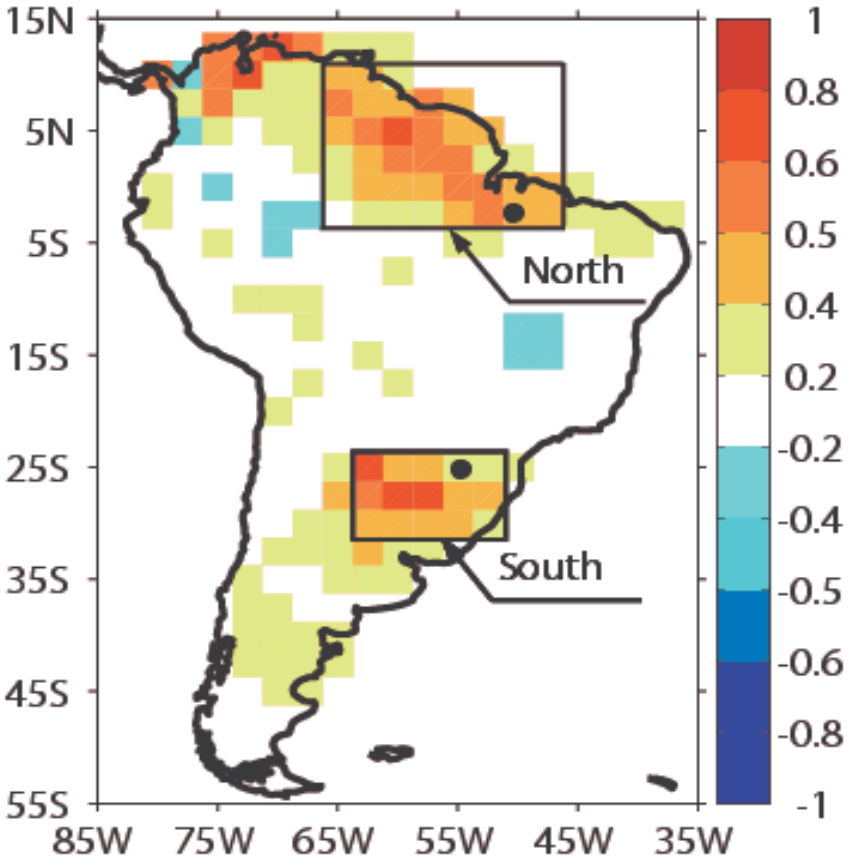

Figure 1. Correlation map of 3-month lead November-December-January 1959-2001 multi-model rainfall anomaly predictions. The multi-model is composed by three DEMETER coupled models (ECMWF, UKMO and Météo-France). Multi-model predictions are obtained by computing the mean of the 27 member ensemble (9 members of each coupled model). The map shows correlations between observed and predicted anomaly time series at each grid point. The north and south boxes are South American regions where regional downscaling of rainfall is performed. The dot inside the north box shows the location of Tucuruí hydropower station (3.75°S; 49.68°W). The dot inside the south box shows the location of Itaipu hydropower station (25.43°S; 54.60°W).

These forecasts are important for national electricity generation management and planning. A Bayesian procedure, referred to here as *forecast assimilation* (Stephenson *et al.* 2005; Coelho 2005), is used to combine and calibrate the rainfall predictions produced by three climate models. Forecast assimilation is able to improve the skill of 3-month lead November-December-January multi-model rainfall predictions over the two South American regions (Figures 2 and 3).

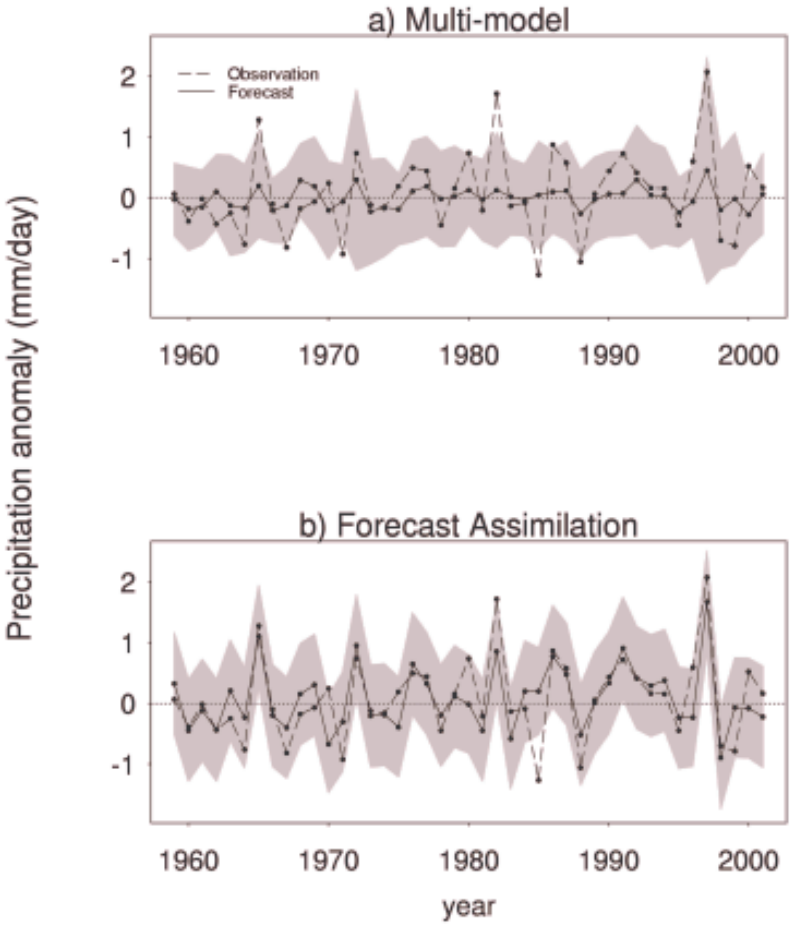

Figure 2. a) Multi-model (i.e. raw, uncalibrated predictions) and b) forecast assimilation 3-month lead November-December-January 1959-2001 cross-validated seasonal mean rainfall anomaly forecasts (in mm/day) for the south box of Figure 1. Mean predicted anomaly (solid line), observed anomaly (dashed line) and the 95% prediction interval (grey shading).

Improvements are noted in forecast seasonal mean values and uncertainty estimates (Table 1). River flow forecasts are less skilful than rainfall forecasts (Figure 4 and Table 2). This is partially because natural river flow is a derived quantity that is sensitive to hydrological as well as meteorological processes, and to human intervention in the form of reservoir management. The full text containing detailed descriptions of the results shown here has recently been published in Meteorological Applications (Coelho *et al.* 2006). Forecast assimilation is planned to be used as part of an integrated seasonal forecasting system for South America (Coelho *et al.* 2005) during the EUROBRISA project (A EURO-BRazilian Initiative for improving South American seasonal forecasts http://www.met.reading.ac.uk/~swr01cac/EUROBRISA/)

Forecast	MSE [x 10^6 $(m^3/s)^2$]	Correlation	Uncertainty [m^3/s]	Brier Score
Paraná river	12.5	0.16	2300	0.25
Tocantins river	7.8	0.29	2200	0.22

Table 2. Skill and uncertainty measures of 3-month lead November-December-January 1959-2001 flow anomaly forecasts for the Paraná and the Tocantins river. Mean squared error (MSE) in $(m^3/s)^2$, correlation, mean predicted uncertainty in m^3/s, and Brier score for the event 'rainfall anomaly less than or equal to zero'.

Acknowledgements
We wish to thank the DEMETER project for making available the coupled model hindcasts used in this research. CASC was sponsored by Conselho Nacional de Desenvolvimento Científico e Tecnológico (CNPq) process 200826/00-0. CASC and FJDR were supported by ENSEMBLES (GOCE-CT-2003-505539).

Figure 3. a) Multi-model (i.e. raw, uncalibrated predictions) and b) forecast assimilation 3-month lead November-December-January 1959-2001 cross-validated seasonal mean rainfall anomaly forecasts (in mm/day) for the north box of Figure 1. Mean predicted anomaly (solid line), observed anomaly (dashed line) and the 95% prediction interval (grey shading).

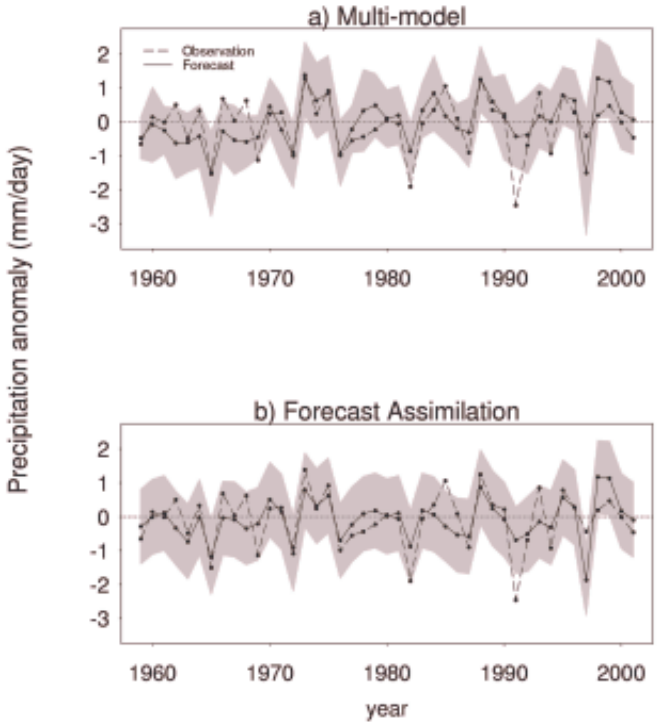

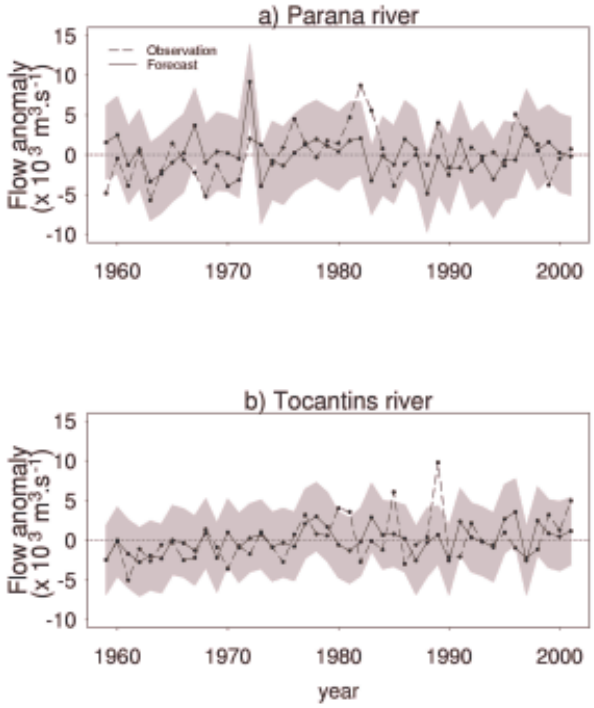

Figure 4. a) Paraná river at Itaipu (25.43°S 54.60°W) and b) Tocantins river at Tucuruí (3.75S, 49.68W) 3-month lead November-December-January 1959-2001 cross-validated seasonal mean flow anomaly forecasts (in m^3/s) obtained with forecast assimilation (solid line). Observed anomalies are represented by the dashed line. The 95% prediction interval is represented by the grey shading.

References

Coelho, C. A. S., Stephenson, D. B., Doblas-Reyes, F. J., Balmaseda, M., Guetter, A. & van Oldenborgh, G. J. (2006) A Bayesian approach for multi-model downscaling: Seasonal forecasting of regional rainfall and river flows in South America. *Meteorological Applications*, 13, 73-82.

Coelho, C. A. S. (2005) Forecast calibration and combination: Bayesian assimilation of seasonal climate predictions. *Ph D. Thesis*. Department of Meteorology, University of Reading. 178 pp.

Coelho, C. A. S., Stephenson, D. B., Balmaseda, M., Doblas-Reyes, F. J. & van Oldenborgh, G. J. (2005) Towards an integrated seasonal forecasting system for South America. *ECMWF Technical Memorandum*, No. 461: 26 pp. Available at: http://www.ecmwf.int/publications/library/do/references/list/14. Also in press in the Journal of Climate.

Stephenson, D. B., Coelho, C. A. S., Doblas-Reyes, F. J. & Balmaseda, M. (2005) Forecast Assimilation: A unified framework for the combination of multi-model weather and climate predictions. *Tellus* 57A: 253-264.

The main features of the 20th Century climate as simulated with the SXG coupled GCM

S. Gualdi, E. Scoccimarro, A. Bellucci, A. Grezio, E. Manzini, and A. Navarra*
Istituto Nazionale di Geofisica e Vulcanologia
Via Donato Creti 12, 40128 Bologna, Italy

1. Introduction

This paper summarizes, very shortly, the formulation and simulation characteristics of the new global coupled climate model, developed over the last few years at the Istituto Nazionale di Geofisica e Vulcanologia (INGV), with the aim of investigating the features and the mechanisms of the climate variability and change. The model, named SINTEX-G (SXG), is an evolution of the SINTEX and SINTEX-F models (Gualdi et al., 2003a, 2003b; Guilyardi et al., 2003, Luo et al. 2004). The ocean component is OPA 8.2 (Madec et al., 1999) with the ORCA2 configuration: 2°x2° cos(latitude) with increased meridional resolutions to 0.5° near the equator, 31 vertical levels with 14 lying in the top 150 meters. The turbulent kinetic energy (TKE) determines the vertical mixing. The evolution of the sea-ice is described by the LIM (Louvain-La-Neuve sea-ice model; Fichefet and Morales Maqueda, 1997, 1999), which is a thermodynamic-dynamic snow sea-ice model, with three vertical levels (one snow and two ices). The ice momentum equation is solved on the same horizontal grid as the ocean model.

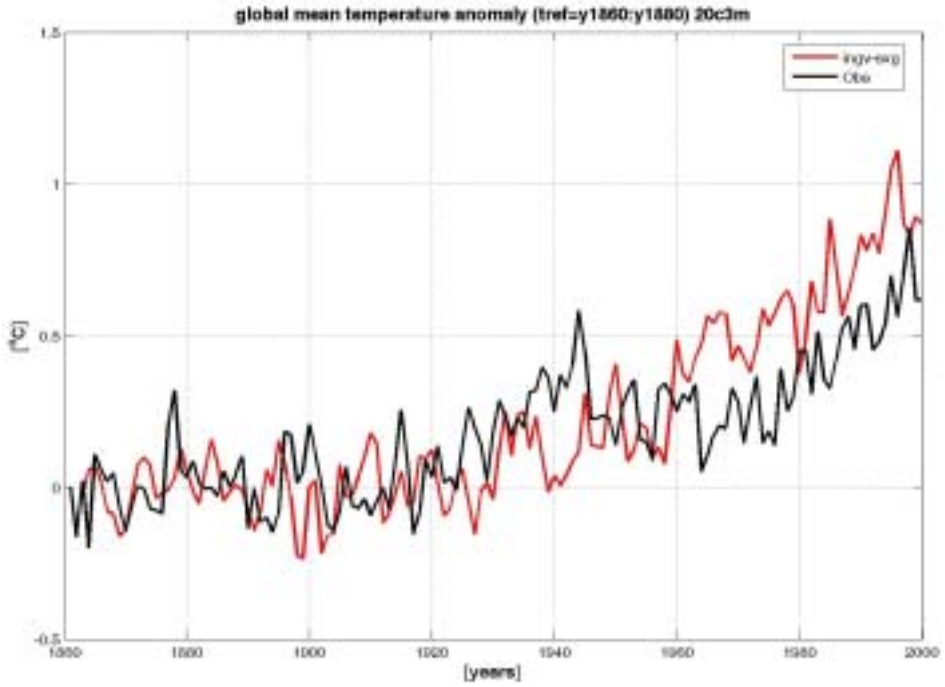

Figure 1: annual mean anomalies of the surface temperature global average for the model (red curve) and observations (back curve, IPCC data). The anomalies are computed with respect to the 1860-1880 mean.

***Corresponding author address:**
Silvio Gualdi
Istituto Nazionale di Geofisica e Vulcanologia
Via Donato Creti 12, 40128 Bologna, Italy
E-mail: gualdi@bo.ingv.it

The atmospheric component is ECHAM4 (Roeckner, 1996) with a T106 horizontal resolution (about 1.125°x1.125°) and 19 hybrid sigma-pressure levels. A mass flux scheme (Tiedtke, 1989) is applied for cumulus convection with modifications for penetrative convection according to Nordeng (1994). The coupling information, without flux corrections, is exchanged every two hours by means of the OASIS 2.4 coupler (Valcke et al., 2000).

With respect to the previous version of the model, SINTEX and SINTEX-F, SXG includes a model of the sea-ice, which allows the production of climate scenario experiments. Here, we present a preliminary analysis of the model results obtained from a simulation of the 20th Century. The experiment has been conducted integrating the model with forcing agents, which include greenhouse gases (CO2, CH4, N2O and CFCs) and sulfate aerosols, as specified in the protocol for the 20C3M experiment defined for the IPCC simulations (http://www-pcmdi.llnl.gov/ipcc/about_ipcc.php). The integration starts from an equilibrium state obtained from a long coupled simulation of the pre-industrial climate, and has been conducted throughout the period 1860-2000. Here, we show mainly results from the period 1958-2000, which are compared with the results obtained from the ERA-40 reanalyses produced at the ECMWF (more information available in http://www.ecmwf.int/research/era), the HadISST1.1 Global Sea-Ice and Sea-Surface Temperature (Rayner et al. 2000) data set (hereafter HadISST), the CMAP precipitation data set (Xie and Arkin, 1997, which are available only for the period 1979-2000). Hereafter, for the sake of simplicity, we will refer to both observational data sets and re-analyses simply as «the observations».

See Figure 2 on the cover page

2. Results

a) Model drift and mean state

The annual mean values of the surface temperature field averaged over all latitudes and longitudes, for the period 1860-2000, is shown in Figure 1 for the model simulation and observations. The curves represent the deviation of the annual mean surface temperature with respect to the 1860-1880 mean, for the period 1860-2000. The observations (black curve) show the well known global warming trend of about 0.6°C over the past century. The model simulation (red curve) exhibits a similar trend, though slightly more pronounced, over the same period. Analogous results are found for the sea-surface temperature (SST) field (not shown).

In order to show the ability of the model to reproduce the main features of the observed mean state of the 20th Century climate, Figure 2-8 show the seasonal means of SST, precipitation, zonal component of the low-level and upper tropospheric wind, sea-ice cover and the stationary waves (eddy 500-hPa geopotential height). Overall, the model appears to capture the basic characteristics of the mean fields, though important differences remain.

In the SST case, Figure 2, coastal upwelling regions in the eastern part of the basins, for example, are often underestimated. Moreover, in the central and eastern South Pacific, the models tend to be too warm. The cold tongue penetrates too far into the west Pacific and the SST patterns are too much symmetrical around the equator. These problems were affecting the mean climate also of SINTEX and SINTEX-F and they are a common feature of many coupled GCMs, which might be related to an inadequate representation of atmospheric convection and to the underestimated model cloud off the Peruvian coast.

Figure 3 shows the climatological precipitation as obtained from the Xie-Arkin (1997) data set and the mean fields obtained from the models for the JFM and JAS season. During the northern winter, the observed precipitation (panel a) exhibits a large belt of high values which extends from the tropical Africa, over the southern Indian Ocean, Indonesian region and northern Australia, up to the Southern Pacific Convergence Zone (SPCZ). A second region of intense precipitation is found over the tropical South America, extending eastward along the equator. Between the equator and about 10°N, a zonal band of intense precipitation extends over most of the Pacific and the Atlantic Inter-Tropical Convergence Zone (ITCZ), with an interruption

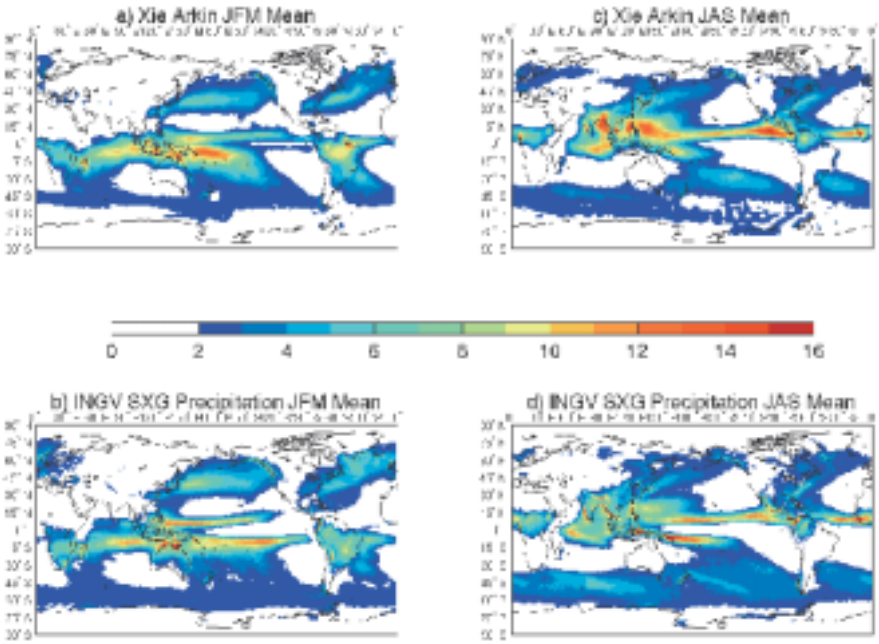

Figure 3: as in Figure 2 but for precipitation. The observations are from the CMAP (Xie and Arkin, 1997) data set.

over the eastern Pacific and equatorial America. At higher latitudes, the signature of the storm tracks is visible over both the central-western Pacific and Atlantic oceans.

The model (panel b) seems to reproduce a reasonably realistic winter precipitation over the extra-tropical oceans in the Northern Hemisphere, and over the tropical Africa, Indian Ocean and Indonesian region. Also over South America, the simulated patterns appears to capture the main basic features of the observed field, though the model tends to shift southward the maximum rainfall observed over the Brazilian Nordeste and the equatorial western Atlantic. In the tropical Pacific, the model exhibits important discrepancies with respect to the observations. The simulation, in fact, clearly overestimates the precipitation over the central-eastern Pacific, south of the equator. Also the structure of the SPCZ is not well simulated. The model produces a sort of southern ITCZ, which lies parallel to the equator. The rainfall over the western equatorial Pacific, on the other hand, is clearly underestimated by the model, probably due to the too cold water simulated in this region (Figure 2). Too cold SST, in fact, might lead to a stabilization of the atmosphere above this portion of the ocean, and consequently reduced precipitation. The rainfall patterns obtained with ECHAM-4 forced with observed SSTs do not show any tendency to produce a double ITCZ in the tropical Pacific (e.g., Roeckner et al. 1996). This suggests that the errors found in the coupled simulations are most likely related to the problems found in the simulated SST patterns (Figure 2).

Figure 4: as in Figure 2 but for the 850-hPa zonal wind. The observations are from the ERA-40 re-analysis data set. The thick, balck line indicates the 0 line countour.

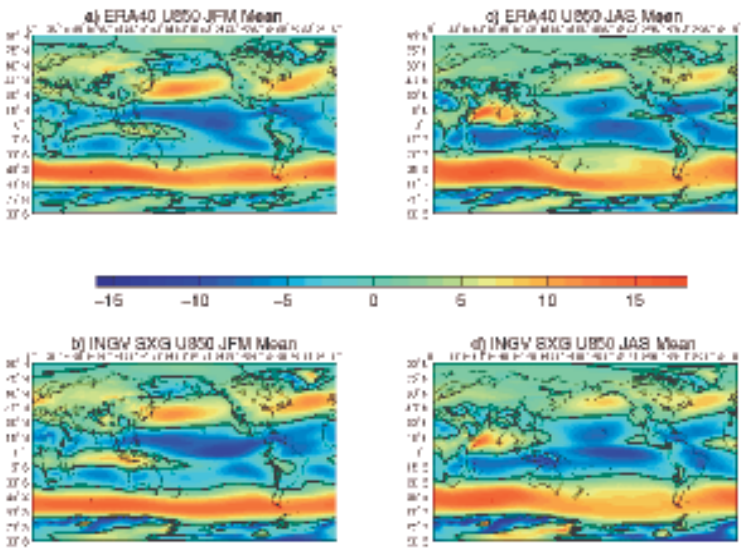

During the northern summer, consistently with the seasonal cycle, patterns of intense precipitation are located north of the equator (Figure 3, panel c). The model appears to simulate quite well the precipitation over the ITCZ band (Figure 3, panel d), across the tropical Pacific and Atlantic oceans. Simulated precipitation over the SPCZ is now reduced, in good agreement with the observations. Also, reasonably realistic patterns of intense rainfall are reproduced over the Congo and Amazonian basins. However, the model rainfall is too weak over the equatorial western Pacific, which is likely caused by the too cold SST found in this region (Figure 2, panel d) and over the region of the Asian summer monsoon.

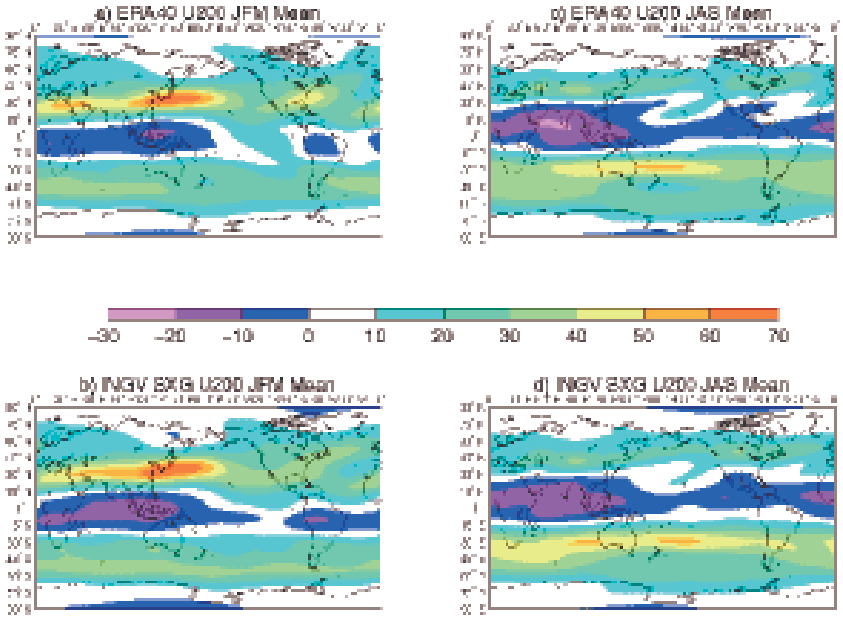

Figure 5: as in Figure 2 but for the 200-hPa zonal wind. The observations are from the ERA-40 re-analysis data set

The underestimation of the Asian summer monsoon is a well known problem of ECHAM-4 (Roeckner et al. 1996). Similarly in the coupled simulation, the precipitation over the areas of the Asian summer monsoon activity appears to be problematic. The model has problems in simulating the maxima of precipitation observed over the Bay of Bengal, the South China Sea and over and to the west of the Philippines. Interestingly, the relatively high-resolution of the atmospheric component makes the model able to reproduce some detail of the precipitation field related to the orographic effects. Thus, for instance, the model is able to simulate the maximum of rainfall over the Western Ghats (Figure 3, panel d).

The zonal component of the near-surface wind is shown in Figure 4 both for JFM and JAS. In general, the model captures the overall features of the low-level zonal circulation, such as, for example, the dominant westerlies in the Extra-Tropics and the mean easterlies (trade winds) in the tropical belt. During northern winter (Figure 4, panels a and b) the storm tracks in the northern mid-latitude are reasonably well reproduced by the simulation, though the intensity of the westerlies is weaker than in the ERA40.

Also the seasonal cycle over the tropical Indian Ocean is well simulated by the model. During boreal winter, the Indian Ocean is dominated by mean easterlies north of the equator, westerlies between the equator and 15°S, and again easterlies in the Southern Hemisphere subtropics. During boreal summer (Figure 4, panels c and d), this pattern changes substantially. North of the equator, the mean flow becomes westerly, with a relatively strong jet over the Arabian Sea (Somali Jet). South of the equator the mean flow is characterized by dominant easterlies. The model reproduces well the main features of these seasonal changes in the low-level circulation, both in terms of pattern distribution and intensity of the fields. Figure 5 shows the seasonal patterns of the upper troposphere zonal wind. For the JFM season (panels a and b) the overall structure is well captured by the model, though the westerly jet is slightly too strong over the region stretching from Himalaya to the western sub-tropical Pacific, and slightly too weak over the western Atlantic. Also, the tropical easterlies extend too far into the estern Pacific.

During Boreal summer (Figure 5, panels c and d), the model tends to overestimate the upper level jet in the Southern Hemisphere; whereas it underestimates the easterlies in the tropical Indian Ocean, which in the observations are reinforced, compared to the winter patterns, as a consequence of the atmospheric dynamical response to the Asian summer monsoon activity.

The modeled weaker easterly jet in the tropical Indian Ocean is consistent with the weak simulated Asian monsoon precipitation discussed above.

The major difference between SXG and the previous versions of the model (SINTEX and SINTEX-F) is the inclusion of a thermodynamic-dynamic model that describes the evolution of the sea-ice. Therefore it is of interest to assess, at least in a qualitative sense, the ability of the model to reproduce the gross features of the observed sea-ice. To this aim, Figures 6 and Figure 7 show the climatological observed and simulated sea-ice distribution for both winter and summer seasons in the northern hemisphere and southern hemisphere respectively. The observations (Figure 6 and Figure 7, panels c and d) are from the NASA NSIDC (National Snow and Ice Data Center) DAAC (Distributive Active Archive Center). The results indicate that the model captures reasonably well the basic seasonal features of the sea-ice distribution both in the Northern and in the Southern Hemisphere, even if it appears to underestimate the sea-ice concentration during the winter season.

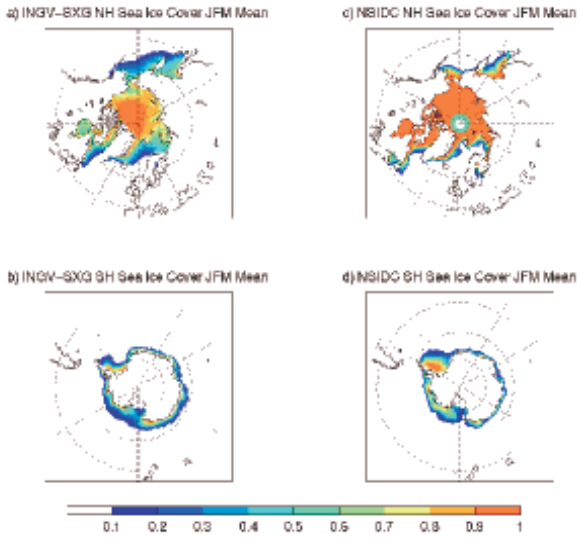

Figure 6: Mean JFM sea ice cover (fraction) from INGV-SXG (1958-2000 period) in the a) Northern and b) Southern Hemisphere, and from the NSIDC NASA dataset (1979-2003 period) in the c) Northern and d) Southern Hemisphere.

Figure 8 shows the observed and simulated stationary waves in terms of the eddy component of the 500-hPa geopotential height (Z500), only for the winter seasons in the respective Hemispheres. Comparing the eddy fields in panels a) and b), the simulated amplitude of the stationary waves is fairly realistic in the Pacific sector, whereas it is slightly overestimated in the Euro-Atlantic region. In the Southern Hemisphere (panels c and d), some difference between model and observations is found in the Pacific southern ocean.

b) Basic features of the mean variability

The seasonal features of the fields shown and described in the previous section exhibit substantial fluctuations over a wide range of time scales. The variability occurring on time scales ranging from seasonal to interannual involves physical phenomena with large impacts both on global climate and social activities, such as, for example, El Niño and the monsoons. Therefore, it is of primary importance that a model be able to reproduce the main features of climate variability on these time scales. A first assessment of the interannual variability can be given by computing the standard deviation of the monthly mean anomalies.

Figure 9 shows the standard deviation of the SST field. During northern winter, in the observations (panel a) the largest variability is located over the equatorial Pacific. This signal is related to the El Niño/Southern Oscillation (ENSO) activity and extends from about the date line to the coast of South America, with a maximum of about 1.2°C located over the equatorial central Pacific. The model (bottom panel), reproduces well the gross pattern of this variability, though the maximum of the singnal appears to be shifted to the east.

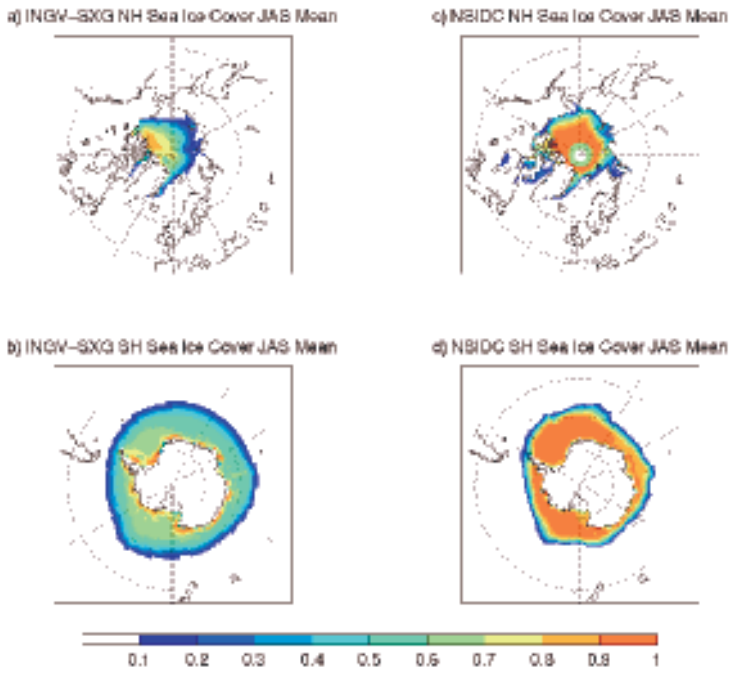

Figure 7: Mean JAS sea ice cover (fraction) from INGV-SXG (1958-2000 period) in the a) Northern and b) Southern Hemisphere, and from the NSIDC NASA dataset (1979-2003 period) in the c) Northern and d) Southern Hemisphere.

During northern summer (panels c and d), both in the observations and in the model the maximum of tropical SST variability has moved from the central Pacific to the region off the coast of South America. In the tropical Indian Ocean, the model appears to overestimate the variability in the eastern part of the basin,off the coast of Sumatra. This varibility is associated with the so-called Indian Ocean Dipole Mode (IODM). Thus, the results shown in Figure 9 suggest that in the model the IODM tends to be excessively active. This finding is consistent with the results that Gualdi et al. (2003) and Fischer et al. (2005) found with the SINTEX model.

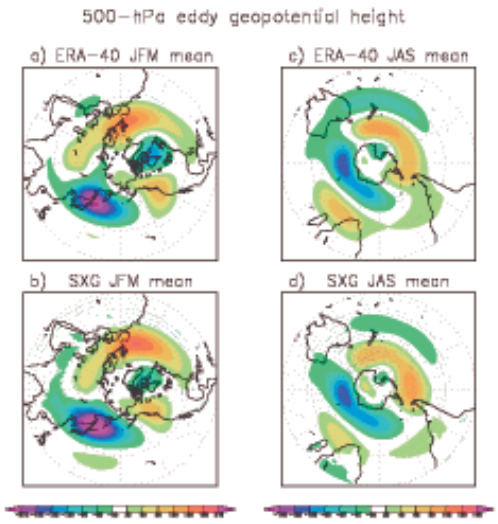

Figure 8: eddy component of the 500 hPa geopotential height (m) from ERA40 re-analysis JFM mean (panel a) and JAS mean (panel c), and from INGV-SXG JFM mean (panel b) and JAS mean (panel d). Countours are 30 metres for the JFM means (left panels) and 20 metres for JAS means (right panels).

A commonly used index for ENSO studies is the time series of the SST anomaly averaged over the so called NINO-3 region (150°W – 90°W, 5°S – 5°N). Such a time series is presented in Figure 10, where 100 years of the model integration is shown. The monthly anomalies have been computed as deviations from the mean annual cycle. The time series exhibits a slight drift of about 0.5°C over the entire period. Overall, the amplitude of the simulated NINO-3 SST anomaly is comparable to the observed one (not shown).

References

Fichefet T., and M. A. Morales Maqueda (1997), Sensitivity of a global sea-ice model to the treatment of ice thermodynamics and dynamics, *J. Geophys. Res.*, **102**, 12,609-12646.

Fichefet T., and M. A. Morales Maqueda (1999), Modelling the influence of snow accumulation and snow-ice formation on the seasonal cycle of the Antarctic sea-ice cover, *Clim. Dyn.*, **15**, 251-268.

Fischer, A., P. Terray, E. Guilyardi, S. Gualdi, and P. Delecluse, 2005: Triggers for the Indian Ocean Dipole/ Zonal Mode and links to ENSO in a constrained coupled GCM. J. Clim, **18**, 3428-3449.

Gualdi, S., E. Guilyardi, A. Navarra, S. Masina, and P. Delecluse (2003a), The interannual variability in the tropical Indian Ocean as simulated by a CGCM, *Clim. Dyn.*, **20**, 567–582.

Gualdi, S., A. Navarra, E. Guilyardi, and P. Delecluse (2003b), Assessment of the tropical Indo-Pacific climate in the SINTEX CGCM, *Ann. Geophys.*, **46**, 1 – 26.

Guilyardi, E., P. Delecluse, S. Gualdi, and A. Navarra (2003), Mechanisms for ENSO phase change in a coupled GCM, J. Clim., 16, 1141–1158.

Luo, J.-J., S. Masson, S. Behera, P. Delecluse, S. Gualdi, A. Navarra, and T. Yamagata (2003), South Pacific origin of the decadal ENSO-like variation as simulated by a couplet GCM. *Gephys. Res. Lett.*, **24**, doi: 10.1029/ 2003GL018649

Madec, G., P. Delecluse, M. Imbard, and C. Levy (1999), OPA 8.1 Ocean General Circulation Model reference manual, Internal Rep. 11, Inst. Pierre-Simon Laplace, Paris, France.

An important feature of ENSO is its seasonal character. In agreement with the observations, the largest model SST anomaly, both negative and positive, in the eastern equatorial Pacific are generally found during northern winter.

Another important characteristics of the ENSO variability is the frequency of the oscillation.

A spectral analysis of the model NINO-3 SSTA time series shown in Figure 10 has been performed (not shown). The simulated ENSO spectrum exhibits a dominant broad peak centered at about 5 years and a secondary, substantially weaker, peak that ranges between 2 and 3 years.

These results are in very good agreement with the results obtained from the observed NINO-3 index.

3. Summary

The major objective of this short article is to give a first, basic assessment of the capability of the SINTEX-G (SXG) coupled model to simulate the main, gorss features of the mean climate and its interannual variability. SXG is the evolution of the SINTEX coupled model, which has already been shown to be able to give a realistic representation of climate and its variability in a number of previous works (e.g., Gualdi et al. 2003a, Gualdi et al. 2003b, Guilyardi et al. 2003, Luo et al. 2003, Gualdi et al. 2005, Masson et al. 2005, Sperber et al. 2005). With respect to the previous versions, SXG differs for the inclusion of a sea-ice model. This makes SXG suitable for climate scenario simulations.

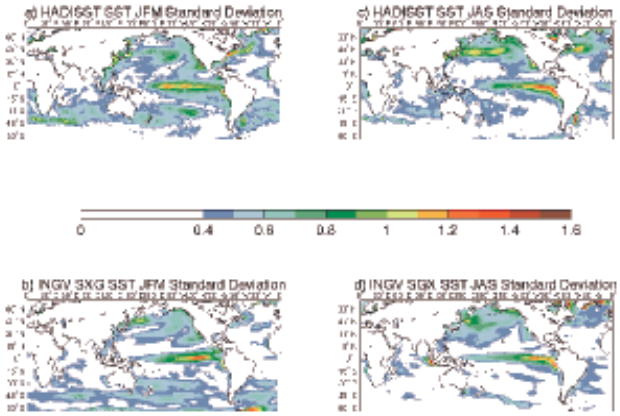

Figure 9: Standard deviation of sea surface temperature (in °C) for 1958-2000 from HADISST a) JFM and c) JAS and INGV-SXG b) JFM and d) JAS.

Here we have shown results obtained from a 20th Century run performed following the 20C3M experiment protocol designed by the PCMDI for the IPCC runs. The results shown indicate that SXG is able to simulate a reasonably realistic mean state and variability. In general, the major model shortcomings, such as for instance the tendency to produce a douple ITCZ in the tropical Pacific, are a common feature of many coupled GCM. These problems, already detected in the SINTEX and SINTEX-F models, are most likely related to an inadequate representation of atmospheric convection.

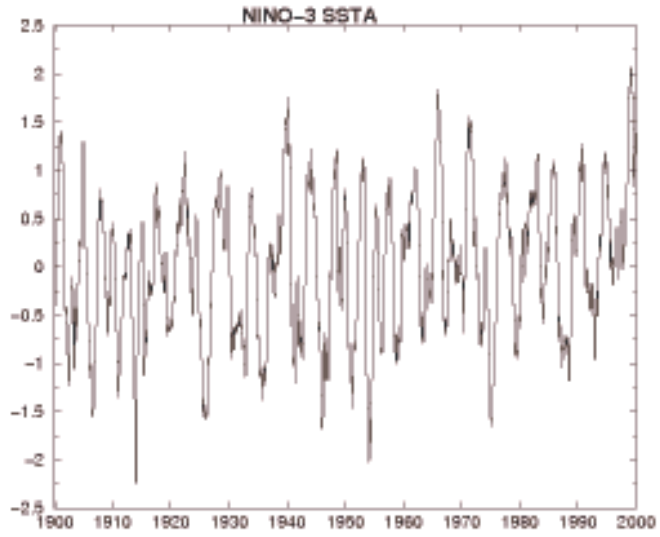

Figure 10: NINO-3 index time series obtained from the SXG model for the XXth Century simulation. The index is computed by averaging the SST anomaly over the so-called NINO-3 region, i.e. 5°S-5°N and 150°W-90°W. The values on the y-axis are SST anomalies in °C.

References (cont.)

Nordeng, T. E. (1994), Extended versions of the convective parameterization scheme at ECMWF and their impact on the mean and transient activity of the model in the tropics, Tech. Memo. 206, Eur. Cent. For Medium-Range Weather Forecasts, Reading, UK.

Roeckner, E. (1996), The atmospheric general circulation model ECHAM-4: Model description and simulation of present-day climate, Tech. Rep. 218, 90 pp., Max-Planck-Inst. fuer Meteorol., Hamburg, Germany.

Tiedtke, M. (1989), A comprehensive mass flux scheme for cumulus parameterisation in large-scale models, Mon.Weather Rev., 117, 1779– 1800.

Valcke, S., L. Terray, and A. Piacentini (2000), The OASIS Coupler User Guide Version 2.4, 85 pp., Eur. Cent. for Res. and Adv. Training in Sci. Comput., Toulouse, France.

Xie, P., and P. Arkin, 1997: Global precipitation: A 17-year monthly analysis based on gauge observations, satellite estimates, and numerical model outputs; Bull. Am. Meteor. Soc., 78, 2539-2558.

Dengue transmission modeling and risk assessment under climatic changes

Nicolas Dégallier[1], Charly Favier[1], Christophe Menkes[1], Jean-Philippe Boulanger[1]
Jacques Servain[1], Walter Massa Ramalho[2], Matthieu Lengaigne[1]

[1]IRD-UR182, LOCEAN, UMR 7159, Tour 45-55, 4ème ét. case 100, 4 place Jussieu 75252 Paris Cedex 05, France; [2]Secretaria de Vigilância em Saúde, Ministério da Saúde, Brasília, DF, Brazil

1 The transmission of dengue virus by *Aedes aegypti*

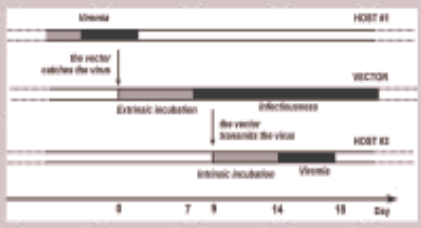

2 The transmission model

The risk of epidemics may be expressed by the basic reproduction number of the disease:

$$R_0 = m\, a^2\, b\, c \exp(-\mu\tau) / \mu\gamma$$

Relative density of mosquitoes
Mean viremia in days
Extrinsic cycle of virus in days
Probability of infecting a man
Probability of infecting a mosquito
Daily mortality rate of vector

R_0 may be expressed as a fonction of the number of pupae by habitant:

$$R_0 = V \bullet N \bullet \frac{S_N \exp(-\mu t_J)}{2 t_N} \bullet \left[\frac{k}{1-\exp(-\mu t_G)}\right] \bullet \exp(-\mu t_E)$$

Number of mosquitoes ready to bite / people
Daily biting rate
Probability of survival at the end of the extrinsic cycle

$$R_0 = V \bullet N \bullet \frac{S_N \exp(-\mu t_J)}{2 t_N} \bullet \left[\frac{k}{1-\exp(-\mu t_G)}\right]^2 \bullet \exp(-\mu t_E)$$

Duration of viremia = 6 days
Survival of pupae = 0.87
Sex ratio = 1.1
Number of blood feeding at each gon. cycle = 1.8

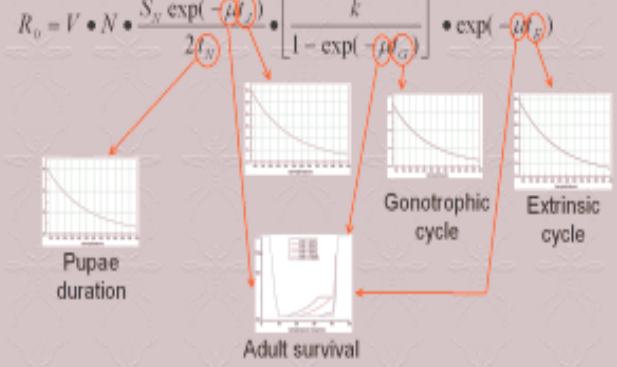

3 The climate models and scenarios

The model has been calibrated with the past and actual extension of dengue

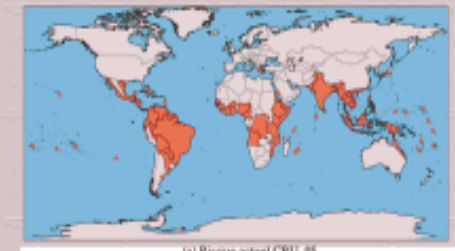

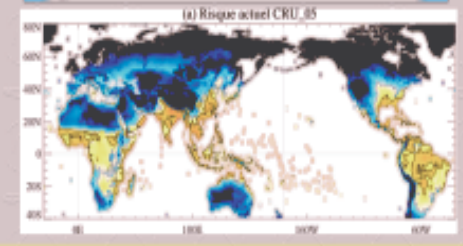

4 2070-2100 mean climates from 12 IPCC models' scenarios used to project Dengue risk. 2 scenarios are presented: SRES B1 (moderate warming) and SRES A2 (extreme)

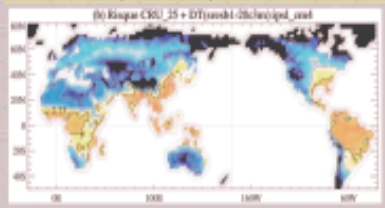

Moderate climate change

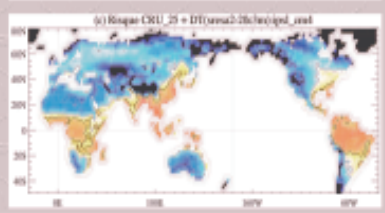

Extreme climate change

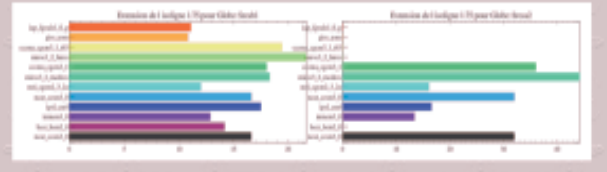

Augmentation of risk areas (%) between actual data and scenarios B1 and A2 with 12 models, respectively

Conclusions: (i) the dengue-transmission risk model is calibrated with parameters which can easily be evaluated experimentally or in the field; (ii) only humidity deficit and monthly mean temperature are necessary to drive the model; (iii) the climatic changes which resulted from very diverse models gave global risk evaluations of the same order (10-20% expansion of risk areas for moderate climate change, and 15-45% for extreme climate change). In the future, environmental and regional spatial parameters will be incorporated in the risk model.

Work supported by: EU CLARIS WP4.2 project; BQR-Université Paris VI; UMR 7159 (IRD-UR 182,CNRS, MNHN, UPMC); MATECLID GICC program.

Training activities on climate variability studies based on MATLAB applications

Andrea F. Carril and Enrico Scoccimarro
Istituto Nazionale di Geofisica e Vulcanologia, INGV, Bologna, Italy

Introduction

This goal of this letter is to document the recent training activities on practical applications for climate variability studies. The course was conducted by Enrico Scoccimarro and Andrea Carril, both with affiliation in the National Institute of Geophysics and Vulcanology (INGV) and it took place in the Department of Atmospheric Sciences at Buenos Aires University (UBA) during February 2006. Local organization also involved people of the Research Centre of the Sea and the Atmosphere (CIMA) who gave support on technical computing issues. The activities were organized in the framework of CLARIS work package 2.1, with the aim of training scientist and graduate students from the South American laboratories in programming languages commonly used in Europe to explore in meteorological time series.

The training activities: short description and first course experiences

The training activities were based on MATLAB (MATrix LABoratory) applications. MATLAB is a high-level language and interactive environment that enables to perform computationally intensive tasks faster than with traditional programming languages such as C, C++ and Fortran (http://www.mathworks.com/products/matlab/). On the one hand, MATLAB is powerful to perform exploratory calculations based on its large built-in mathematical internal functions. On the other hand, it is user friendly, working like a debugger that gives an intermediate answer after every single interrogation, making possible to build the user-own codes checking the progresses step by step.

MATLAB is an extraordinary tool to conduct analysis of climatological datasets. It is flexible to perform simple computations (as e.g., the calculation of seasonal anomalies) or complex statistical analysis (as e.g., singular value decomposition, Fourier analysis) and to graphically display the computations result in the successive step of the user's script (e.g. by plotting time series, contour maps, histograms; Figure 1, see page 18). The course, made by 5-session of 3-hour each one, was projected by Scoccimarro and Carril (2006) focusing on applications to study issues related with the climate variability and climate change. The training sessions were designed assuming that students had a general knowledge of statistics. Although the activities were primarily intended for graduate students in atmospheric or ocean sciences, a number of experienced researchers also took part of the initiative.

Because students and educators were coming from diverse countries (Argentina, Brazil, Chile, France, Italy and Uruguay) all the five training sessions were taught in the short period of one week. Lessons were during the mornings and diverse exercises proposed as homework were discussed when required by individual groups during the successive morning. An educational kit containing a number of documentation files, demonstration scripts and datasets to be managed during the training time, the list of proposed exercises and a set of INGV-built specific functions for climate variability studies was distributed during the first morning and installed in the laptops of the participants. The modality of the course was interactive. Students were arranged into groups of about 3-people sharing one laptop with the educational kit installed. After introducing the theory of a particular subject, the students were pushed to practicing on it, based on a list of proposed exercises and/or changing the settings of some pre-built scripts.

During the first session, the students were introduced to the MATLAB. As a first step, the working environment was presented and emphasis was on learning how to handle matrixes. Then, the most useful functions were listed and the students had their first experiences entering explicit list of elements and working interactively with those simple vectors or/and matrixes. In successive steps, the students were instructed to load matrixes from external data files, to operate and to save the matrixes in an output file. In particular, loading and saving was exercised reading and writing datasets in different formats: MATLAB, netcdf, ascii and binary (sequential and access direct) format. Although we deal with some unexpected problems related with the different versions of MATLAB and/or netcdf libraries installed in the laptops of the participants, thanks to the assistance of Alfredo Rolla (CIMA) heterogeneities were solved and students were able to run the first demonstration scripts with success.

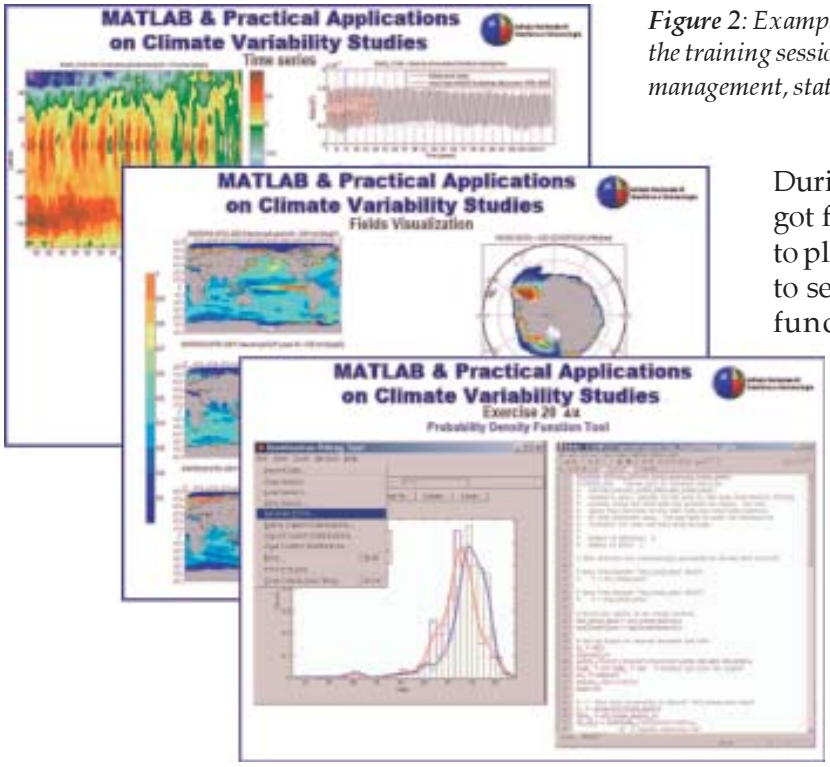

***Figure 2**: Example of typical exercises carried out during the training sessions, including scripts programming, data management, statistical computations and visualization.*

During the second day, the students got familiar with some basic settings to plot time series, learned about how to set a script properly, how to build functions that includes dynamic number of arguments and they were introduced on logical conditions. At the end of the second session, and after providing the students some elements of code vectorization, they studied the performance of a series of scripts programmed with different levels of vectorization. At the end of the second session, most of the working groups were successful on understanding the MATLAB philosophy and to operate in a vectorial approach, changing indexation when required and avoiding the typical «loops» used in other languages as e.g., Fortran.

A number of demonstrations focusing on diverse diagnostics and statistical tools for specific climate studies were performed during the third and fourth sessions. The starting point was the management of time series, performing some basic statistic as the estimation of means, raw anomalies, seasonal dependent anomalies, standard deviation, time series correlations and the computation of particular climatic indexes as e.g., the Southern Oscillation Index (SOI) and the Niño 3 index. The exercises were done using diverse datasets from the educational kit, coming from reanalysis data and climate model simulations. Students got also practiced on detrending single time series and time series from ensemble experiments, and on filtering time series by setting low pass, band pass and high pass filters. In particular, they were able to estimate and plot correlation maps from filtered time series (according to a certain level of statistical significance), verifying the global coupling between the global sea surface temperatures (SST) and the sea level pressure (SLP) fields, on different time scales. They also managed the scripts to plot Hovmöller diagrams of specific patterns of SST anomalies over the Southern Ocean, on the interannual time scale (i.e., they built the Antarctic Circumpolar Wave). The participants were initiated on the interpolation of fields from regular and irregular grids. The examples were based on SST fields discretized in a T106 Gaussian grid and in the non parametric grid illustrated in Figure 3 (a particular ocean model grid). After that, a large attention was on the computation

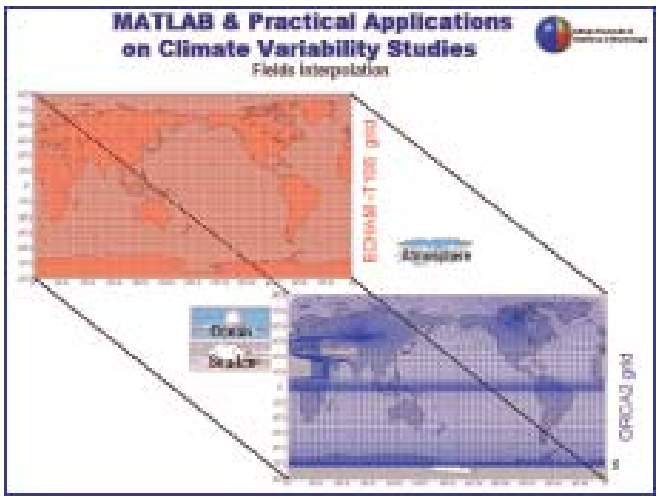

***Figure 3**: Example of typical interpolations when using climate model fields. Input dataset is given in a T106 Gaussian grid while the discretization of the output data is according to a curvilinear grid with two poles in the Northern Hemisphere.*

of leading modes of climate variability, based on the singular value decomposition (SVD) of matrixes. Students were running a series of INGV-built scripts with diverse degree of complexity, to perform empirical orthogonal functions (EOF), varimax rotation and combined EOF. Unfortunately, when students were exploring into the pre-built scripts to perform complex EOF, problems related with the RAM memory of some laptops come along. In those cases, the exercitation was not possible. If teaching new training sessions, some extra efforts are necessary to reduce the memory requested for some pre-built scripts to ensure a good performance over a wide spectrum of machines. Signal processing in the climate system was illustrated by describing diverse approaches to the spectral and wavelet analysis, applied to El Niño 3 time series. Finally, last scheduled exercitation was regarding density probability functions. The exercise was done by exploring in a dataset made by time series of SST values in the eye of n-hurricane from a pre-industrial run conducted using the INGV model. In that case, the students were instructed about how to get useful information to programming scripts by exploring interactively in a graphical user interface.

Last session was a free-programming morning. Every group was requested to elaborate and execute a plan of work according to their own interests; the tutors were helping the individual groups on solving problems. The experience we got during the first training course is that optimum results were reached by those working groups made by one experienced researcher and two graduate students. Researchers were able to extrapolate their Fortran programming experience and vectorizate their codes quickly, according to the MATLAB philosophy (experience that was in general missing in those working groups made by graduate students only).

Acknowledgements

Andrea Carril and Enrico Scoccimarro give thanks to the Department of Atmospheric Sciences (Buenos Aires University) for providing the physical space and for the local organization. They also appreciate the technical support by the system manager of the Research Center of the Sea and the Atmosphere (CIMA). Special thanks to Jean Philippe Boulanger, Mario Nuñez, Paula Richter, Alfredo Rolla and Matilde Rusticucci. Last but not least, many thanks to all the students! The success of the course was mainly due to the great enthusiasm of its participants.

References: Scoccimarro E. and A. F. Carril, 2006: MATLAB and Practical Applications on Climate Variability Studies. Free educational kit, registered on «Earth Prints Repository» (Italian site) and available on-line at http://hdl.handle.net/2122/1044

CONTENTS

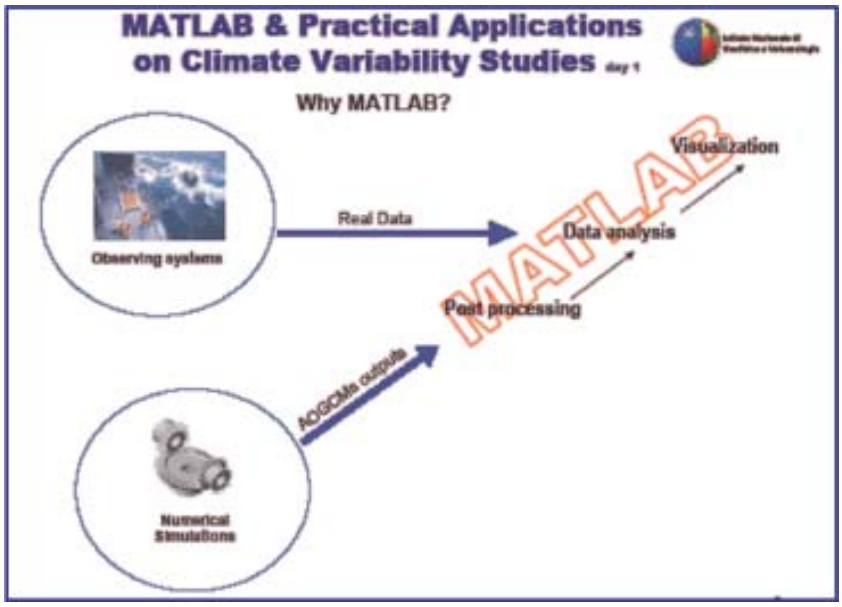

***Figure 1**: MATLAB is capable of performing a wide range of numerical computations and also possess extensive graphics capabilities.*

CLARIS News is published every six months by the CLARIS Project and distributed freely upon request.

Editorial Board: Jean-Philippe Boulanger, Carlos Ereño, Roberto Mechoso and Paula Richter
Layout: Paula Richter & Jean-Philippe Boulanger

CLARIS
c/o Departamento de Ciencias de la Atmosfera - UBA
Pabellón II - 2do piso - Ciudad Universitaria
1428 Buenos Aires - ARGENTINA
Tel: 54 11 4576 3356 or 54 11 4576 3364 ext 20
Fax: 54 11 4576 3356 or 54 11 4576 3364 ext 20
E-mail: clarisproject@cima.fcen.uba.ar
Web site: www.claris-eu.org